Imaging Cortical Anatomy by High-Resolution MR at 3.0T: Detection of the Stripe of Gennari in Visual Area 17

Emmanuel L. Barbier,[1,2] Sean Marrett,[3] Adrian Danek,[4,5] Alexander Vortmeyer,[6] Peter van Gelderen,[1] Jeff Duyn,[1] Peter Bandettini,[3] Jordan Grafman,[4] and Alan P. Koretsky[1*]

The brain can be parcellated into numerous anatomical and functional subunits. The classic work by Brodmann (Vergleichende Lokalisationslehre der Grosshirnrinde in ihren Prinzipien dargestellt auf Grund des Zellenbaues. Leipzig: Barth; 1909) identified areas of the cerebral cortex based on histological differences. An alternative to his cytoarchitectonic approach is the myeloarchitectonic approach. MRI has excellent white/gray matter contrast in the brain due to the presence of myelin, and thus seems uniquely suited for in vivo studies of cortical myeloarchitecture. Here it is demonstrated that the stripe or stria of Gennari can be consistently detected in human occipital cortex. T_1-weighted images obtained at 3T from six of 10 normal volunteers, with resolutions of 350 × 350 × 600 μ, clearly demonstrate this myelin-rich intracortical layer. It is concluded that the striate cortex (area 17 of Brodmann) of the human brain can be delineated in vivo on T_1-weighted images, potentially enabling detection of specific cortical boundaries within individual brains. Magn Reson Med 48:735–738, 2002. Published 2002 Wiley-Liss, Inc.†

Key words: human; cortical architecture; brain maps; myelin; Area V1

A major interest in neuroscience is the parcellation of the brain into anatomically and functionally distinct and relevant areas. The defining work in this field was that of Brodmann (1), who segmented more than 50 cortical areas in the human brain based on local differences of cortical cell layers. Many of these cytoarchitectonic boundaries have been shown to have functional significance on the basis of lesion studies in patients and, more recently, on the basis of in vivo functional imaging techniques. A critical step is to properly correlate sites of increased functional activity with anatomical areas. However, high interindividual variability, as observed by histological techniques (2–4), requires techniques that would enable in vivo parcellation of the individual human brain cortex into specific areas.

Magnetic resonance imaging (MRI) has excellent soft-tissue contrast and can readily distinguish white and gray matter in the brain based on the MRI properties of these tissues (5). Brain regions have been delineated using the myeloarchitectonic approach, which originated in the 18th century (6). Gennari was the first to describe the stria of heavily myelinated cortex in the posterior part of the brain. This is the well-known striate cortex in the visual system. Today, many cortical areas (notably layer IV) are known to show myelin-rich layers. In addition to the striate area or area 17 of Brodmann (7), these areas include V5/MT at the temporo-occipital junction (8,9), and Heschl's gyrus in the temporal lobe (10). The myeloarchitectonic approach enables visualization of the borders of specific areas. For example, the transition zone between Brodmann's areas 17 and 18 is defined by readily detectable changes in Gennari's stripe. Some authors have described MR contrast in the gray matter of the cortex, which was attributed to myelin layers (7,10). However, these observations were limited by spatial-resolution limitations due to low signal-to-noise ratios (SNRs). With the advent of high-field MRI devices for human use, it may be possible to obtain spatial resolutions that enable robust detection of myelinated cortical layers, thus allowing the parcellation of the human brain cortex in vivo for delineating brain regions in individuals. Here we show that MRI at 3T is capable of consistently detecting a myelinated layer of the human calcarine cortex, which can be identified as the stripe of Gennari, in normal volunteers. Because of its location near the brain surface, a surface coil was used to optimize the SNR. Images were obtained with a spatial resolution of 350 × 350 × 600 μ. Prospects for using MRI to determine myeloarchitecture throughout the cortex are discussed based on this work.

MATERIAL AND METHODS

MRI on Normal Volunteer

All of the studies were approved by the National Institute of Neurological Disorders Institutional Review Board and performed in strict accordance with their policies. Ten normal volunteers gave their consent to participate in this study, which was performed on a whole-body 3.0 T scanner (GE Medical Systems) equipped with gradients capable of 40 mT/m and a slew rate of 150 mT/m/s. A volume transmit/surface receive system (Nova Medical, Inc.) was used to acquire the images. The surface coil was placed over the visual cortex so as to maximize the SNR in the

[1]Laboratory of Functional and Molecular Imaging, National Institute for Neurological Disorders and Stroke, National Institutes of Health, Bethesda, Maryland.

[2]Laboratoire mixte INSERM U438, Université Joseph Fourier, RMN Bioclinique, LRC-CEA, Hôpital Albert Michallon, Grenoble, France.

[3]3 Tesla Functional Neuroimaging Facility, National Institutes of Mental Health, National Institutes of Health, Bethesda, Maryland.

[4]Cognitive Neurosciences Section, National Institute for Neurological Disorders and Stroke, National Institutes of Health, Bethesda, Maryland.

[5]Neurologische Klinik, Ludwig-Maximilians-Universität München, Germany.

[6]Molecular Pathologenesis Unit, Surgical Neurology Branch, National Institute for Neurological Disorders and Stroke, National Institutes of Health, Bethesda, Maryland.

E.L. Barbier and S. Marrett contributed equally to this work.

*Correspondence to: Alan P. Koretsky, LFMI/NINDS/NIH, Room 10/B1D118, MSC 1065, Bethesda, MD 20892. E-mail: koretskya@ninds.nih.gov

Received 23 December 2001; revised 14 May 2002; accepted 14 May 2002.
DOI 10.1002/mrm.10255
Published online in Wiley InterScience (www.interscience.wiley.com).

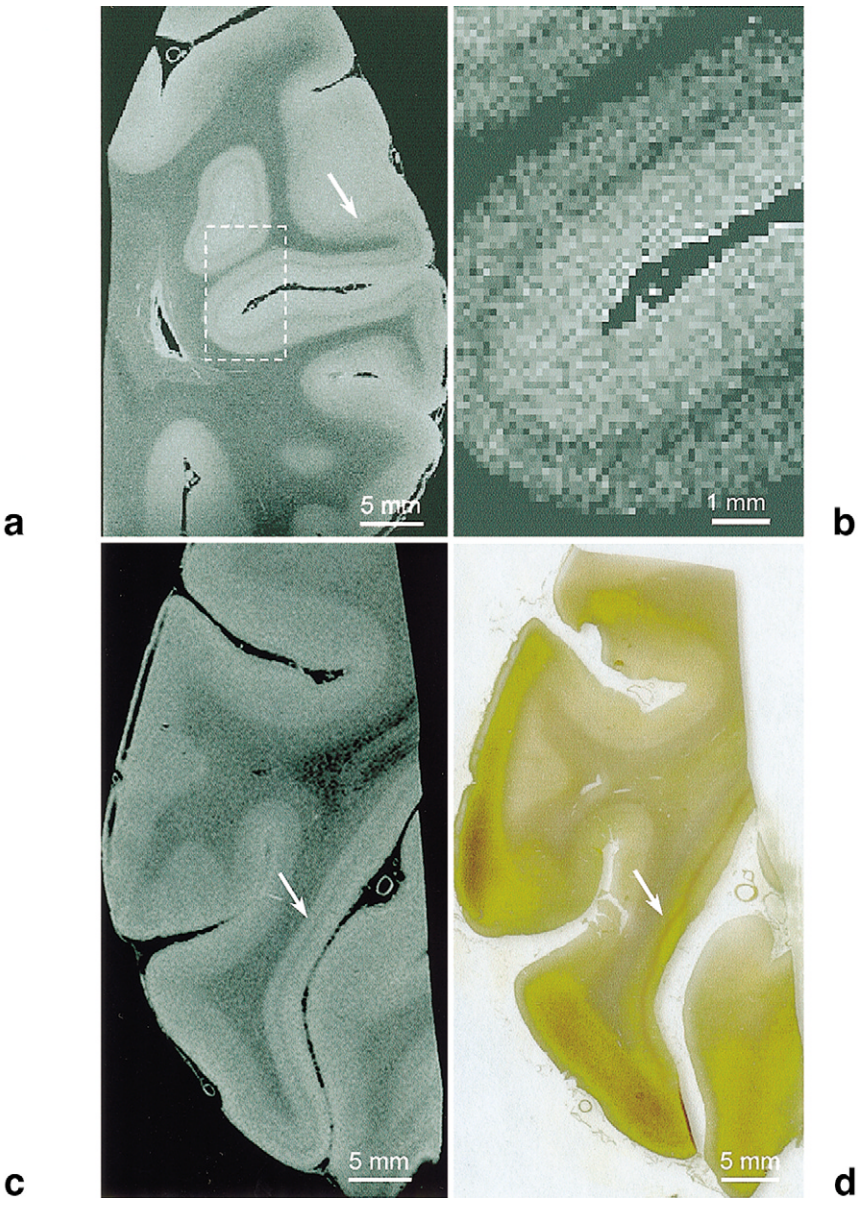

FIG. 1. Images from a 3D dataset acquired on a formalin-fixed human brain sample at 4.7 T, using a spin-echo sequence. The spatial resolution is ~110 μm. **a:** Proton density map. Darker regions within the brighter gray matter are due to myelin. In particular, the thick stripe that starts at the arrow is the Gennari stripe in area 17 of the visual cortex. **b:** Expansion of the area framed by the white rectangle overlaid on part **a**. It can be seen that the width of the Gennari stripe is 2–4 pixels. **c:** Proton density image from a 3D dataset acquired on a second fixed human brain sample at 4.7 T. The spatial resolution is ~110 μm. **d:** A 10-μm-thick histological section stained with Bielschowsky silver stain for myelin, corresponding to (**c**) the MR image. **c** and **d:** The white arrows point to the stripe of Gennari as detected by both MRI and the myelin stain.

area of interest. To maintain head position, a thermoplastic bite bar was used.

After acquisition of scout images, eight high-resolution T_1-weighted 3D datasets were acquired with a spoiled gradient-echo (SPGR) sequence (with an inversion prepulse, TI = 400 ms, TR = 13 ms, TE = 6 ms, bandwidth = 15.63 kHz, flip angle = 19°, FOV = 9 × 9 × 3.7 cm^3, matrix size = 256 × 256 × 62, and one average), yielding images with a spatial resolution of 350 × 350 × 600 μm^3. Each of the eight datasets was acquired in 5 min 17 s, yielding a total scan time of about 45 min.

Each 3D dataset was subsequently processed using the Brain Imaging Software Toolbox (McGill University (11)). First, each dataset was realigned with respect to the first dataset of the series, allowing the software to perform rotations and/or translations in all directions using tricubic interpolation. The registration was driven by the cross-correlation of individual volumes to the first volume in the series. The resampled datasets were then averaged.

MRI and Histology on Fixed Brain Sections

Two samples of visual cortex were obtained from formalin-fixed post-mortem brain in agreement with the guidelines of the NIH Office of Human Subject Research. Samples were placed in a vial containing perfluoropolyether (Ausimont, NJ). Because perfluoropolyether does not contain any protons, it does not contribute to the signal. However, its presence considerably reduces susceptibility artifacts at the edges of the sample.

Samples were imaged on a Bruker BioSpec Avance console operating at 4.7 T with 3D spin-echo sequences using a 25-mm volume coil. The following imaging parameters were used: TR = 4100 ms, TE = 8 × 14 ms, flip angle = 90°, FOV = 56 × 28 × 14 mm^3, matrix size = 512 × 256 × 128, and one average. The acquisition duration was 37 hr 25 min, yielding a spatial resolution of ~110 μm in all directions. The proton density map was computed from this dataset using a two-parameter exponential decay model.

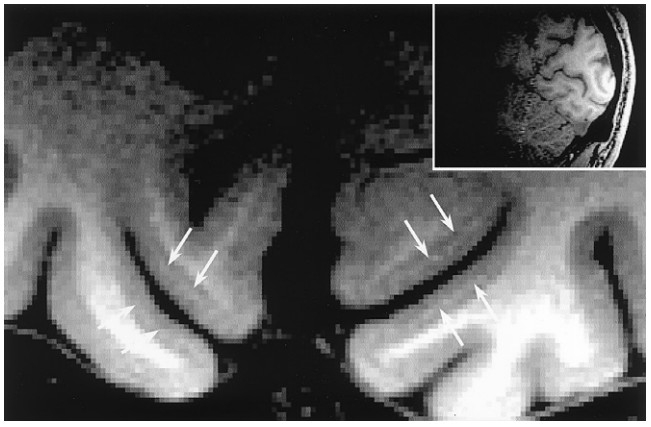

FIG. 2. T_1-weighted MRI (350 × 350 × 600 μm^3 spatial resolution) in the visual cortex, acquired at 3 T. The white arrows point to a thin white line, which we identify as the stripe of Gennari. The insert shows the surface coil coverage on a T_1-weighted sagittal MR image (SPGR with inversion pre-pulse: TI = 400 ms, TR = 13 ms, TE = 6 ms, flip angle = 19°, FOV = 20 × 20 mm^2, slice thickness = 1.2 mm, matrix size = 256 × 256).

After MRI, one of the two brain samples was processed through ethanol and xylene and embedded in paraffin. Sections (10 μ thick) were obtained from the paraffin block, and a Bielschowsky silver stain was performed to visualize the stripe of Gennari.

RESULTS

Figure 1 shows the proton density map obtained from a post-mortem sample of the visual cortex at 4.7 T. Layer IVb, the stripe of Gennari, can readily be visualized as a dark band through some of the cortex. In Fig. 1a, the white arrow points to one end of the stripe, showing the border between Brodmann's area 17 and 18. Figure 1b represents an expansion of the area framed by the white rectangle overlaid on Fig. 1a. It can be seen that the width of Gennari's stripe is 2–4 pixels (i.e., 200–400 μm) for this sample. Figure 1d shows high-resolution MRI of a different fixed brain sample also obtained at 4.7 T using proton density weighting. Figure 1c shows the same section stained with Bielschowsky silver stain. Arrows on the stained section and the MRI indicate the stripe of Gennari running in area 17 of the occipital cortex. The MRI contrast in this case was due to the low proton density in this heavily myelinated area of the cortex.

Figure 2 shows an example of one section of a 3D MRI obtained at 3T from a normal volunteer with a surface coil placed over the visual cortex. The insert shows a sagittal section showing the FOV of the surface coil. Arrows indicate the high-intensity stripe detected from the gray matter in area 17. In this case, after eight averages, the spatial resolution was 350 × 350 × 600 μm. It was difficult to detect the stripe in images with lower spatial resolution, and even at these high resolutions it was difficult to follow the full length of the stripe through multiple planes. Moreover, smoothing the high-resolution images makes the stripe difficult to detect (data not shown).

Figure 3 shows brain images from two additional normal volunteers. For both volunteers, the stripe of myelin can be seen on all consecutive slices detected in the visual cortex. For all of the six volunteers in whom MRI was obtained that was not corrupted by large head movements, the stripe of Gennari could be detected.

DISCUSSION AND CONCLUSIONS

There has been rapid growth of MRI applied to the brain because of its impact on clinical diagnostics and the success of functional MRI (fMRI) in cognitive neuroscience. Indeed the advantages of high-field MRI for fMRI has caused intensive development of 3T MRI devices. The recent FDA approval of a 3T scanner ensures that there will be aggressive development of this type of scanner. The higher field leads to increased signal and (in principle) the ability to image at higher spatial resolutions, as discussed by Callaghan (12). In the present study we used long scan times (~45 min) to obtain very high spatial resolution images of the visual cortex of normal human volunteers. At resolutions of 350 × 350 × 600 μ, a bright stripe running through layer IVb of Brodmann's area 17 could be

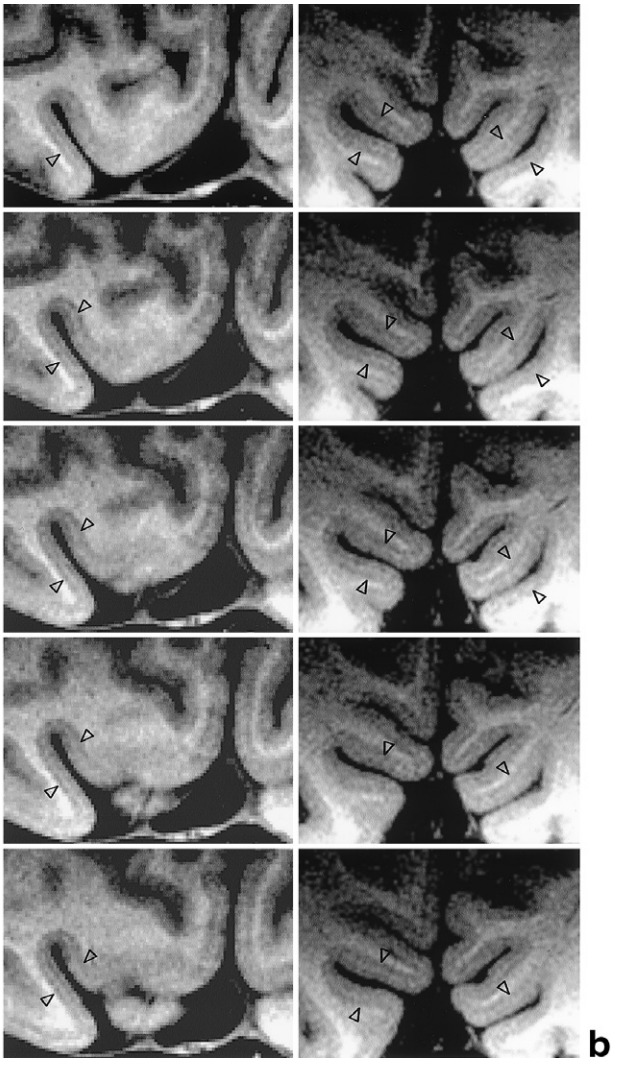

FIG. 3. **a** and **b:** T_1-weighted MR images from two different volunteers, representing contiguous slices in the averaged 3D datasets acquired. For each volunteer and in each slice, the stripe of Gennari can be seen, as indicated by the black open arrows.

detected. We identified this as the stripe of Gennari, which represents myelinated fibers in this area of the brain. Signal intensity was similar to that in other white matter regions, indicating that the contrast was probably dominated by myelin.

There is one previous report of detecting the Gennari stripe by MRI in humans, by Clark et al. (7). In their work, proton-density imaging at 1.5 T was used and images were acquired with a resolution of 390 μm × 390 μm × 3 mm. The proton-density weighting caused the Gennari stripe to appear darker than the surrounding tissue, leading to potential difficulties in distinguishing the stripe from other artifacts that can cause loss of signal on MRI. In comparison, we acquired images from about sixfold-smaller volumes and used T_1 weighting. The T_1 weighting leads to a higher signal in the Gennari stripe. Image acquisition times can be significantly shorter with T_1-weighted sequences compared to proton-density-weighted sequences. Furthermore, Clark et al. (7) used a slice prescription perpendicular to the calcarine to allow for larger voxel sizes (0.460 mm^3 vs. 0.073 mm^3), while our axial slice prescription did not depend on variations in the sulcal anatomy of the subject.

The present in vivo spatial resolution appears to be borderline for clearly following the stripe of Gennari in its continuity and for defining its end because it has only a single pixel width, and in the long axis of the pixel (600 μm length), partial volume effects lead to fuzzy borders. Moreover, at this spatial resolution, head movements become a major issue. In this study a bite bar was used, but this solution may not be the most appropriate, especially in a clinical environment. The Gennari stripe was detected in six of 10 volunteers. In four of the volunteers there were large motion artifacts. It is clear that minimizing motion is crucial for obtaining very-high-resolution MRI. The use of techniques (such as cardiac gating) to minimize motion, more robust ways to hold the head, and improved motion correction techniques should help with this problem.

Recent progress in MRI hardware should provide increased spatial resolution. For example, a 7.0 T scanner yields at least twice the SNR as that from a 3.0 T scanner (13). Moreover, using optimized RF coil arrays in conjunction with multiple receivers has the potential of further improving the SNR (14). An optimistic estimate is that these improvements in SNR may allow 250 × 250 × 250 μm^3 voxels to be acquired within the 45-min scan time used in this study. While these scan times are long compared to typical clinical protocols, the increased anatomical definition should justify the long scan times. With such a high spatial resolution, based on our in vitro images, it should be possible to follow the stripe of Gennari along the Calcarine sulcus and robustly detect changes that define specific brain regions.

The data processing can also be improved—for example, by limiting the FOV to the areas of interest during the registration process. Moreover, even with the image quality obtained in this study, it should be possible to extract most of the stripe by making some simple assumptions, such as regarding the continuity of the stripe, its approximate location, and the absence of sharp changes in directions. This type of assumption has been successfully used in the analysis of diffusion tensor data (15).

Finally, MR can image myelin in many different ways, including methods based on magnetization transfer (16), anisotropy of water diffusion (15), and T_2 or T_2^* weighting (7,17). It is important to determine which contrast mechanism allows the most robust detection of myeloarchitecture in the cortex. Myelin is a marker for other brain structures in addition to area 17, such as area V5/MT (8,9), and the first Heschl gyrus in the primary auditory cortex (10). MRI can be made sensitive to other structural features that might complement myeloarchitectonics. These include microvascular architecture and anisotropic environments. In conclusion, it is possible that the use of high-resolution MRI to detect the myeloarchitecture and other histological features of the brain will enable brain parcellation into anatomically and functionally distinct areas in individual subjects.

NOTE ADDED IN PROOF

Recently, the Gennari stripe in the striate cortex of the monkey has been detected using MRI at 4.7T. This work (18) opens the possibility of performing myeloarchitecture with MRI on non-human primates.

REFERENCES

1. Brodmann K. Vergleichende Lokalisationslehre der Grosshirnrinde in ihren Prinzipien dargestellt auf Grund des Zellenbaues. Leipzig: Barth; 1909.
2. Stensaas SS, Eddington DK, Dobelle WH. The topography and variability of the primary visual cortex in man. J Neurosurg 1974;40:747–755.
3. Murphy GM. Volumetric asymmetry in the human striate cortex. Exp Neurol 1985;88:288–302.
4. Amunts K, Malikovic A, Mohlberg H, Schormann T, Zilles K. Brodmann's areas 17 and 18 brought into stereotaxic space—where and how variable? Neuroimage 2000;11:66–84.
5. Gadian DG. NMR and its applications to living systems, 2nd ed. Oxford: Oxford University Press; 1995. 283 p.
6. Glickstein M. The discovery of the visual cortex. Sci Am 1988;259:118–127.
7. Clark VP, Courchesne E, Grafe M. In vivo myeloarchitectonic analysis of human striate and extrastriate cortex using magnetic resonance imaging. Cereb Cortex 1992;2:417–424.
8. Clarke S, Miklossy J. Occipital cortex in man: organization of callosal connections, related myelo- and cytoarchitecture, and putative boundaries of functional visual areas. J Comp Neurol 1990;298:188–214.
9. Watson JD, Myers R, Frackowiak RS, Hajnal JV, Woods RP, Mazziotta JC, Shipp S, Zeki S. Area V5 of the human brain: evidence from a combined study using positron emission tomography and magnetic resonance imaging. Cereb Cortex 1993;3:79–94.
10. Yoshiura T, Higano S, Rubio A, Shrier DA, Kwok WE, Iwanaga S, Numaguchi Y. Heschl and superior temporal gyri: low signal intensity of the cortex on T2-weighted MR images of the normal brain. Radiology 2000;214:217–221.
11. Collins DL, Neelin P, Peters TM, Evans AC. Automatic 3D intersubject registration of MR volumetric data in standardized Talairach space. J Comput Assist Tomogr 1994;18:192–205.
12. Callaghan PT. Principles of nuclear magnetic resonance microscopy. Oxford: Oxford University Press; 1991. 492 p.
13. Vaughan JT, Garwood M, Collins CM, Liu W, DelaBarre L, Adriany G, Andersen P, Merkle H, Goebel R, Smith MB, Ugurbil K. 7T vs. 4T: RF power, homogeneity, and signal-to-noise comparison in head images. Magn Reson Med 2001;46:24–30.
14. Pruessmann KP, Weiger M, Scheidegger MB, Boesiger P. SENSE: sensitivity encoding for fast MRI. Magn Reson Med 1999;42:952–962.
15. Basser PJ, Mattiello J, LeBihan D. MR diffusion tensor spectroscopy and imaging. Biophys J 1994;66:259–267.
16. Wolff SD, Balaban RS. Magnetization transfer contrast (MTC) and tissue water proton relaxation in vivo. Magn Reson Med 1989;10:135–144.
17. Ogawa S, Lee TM, Kay AR, Tank DW. Brain magnetic resonance imaging with contrast dependent on blood oxygenation. Proc Natl Acad Sci USA 1990;87:9868–9872.
18. Logothetis N, Merkle H, Augath M, Trinath T, Ugurbil K. Ultra high-resolution fMRI in monkeys with implanted RF coils. Neuron 2002;35:227–242.